



Reprint 935

Climatology and Performance of LIDAR-based Visibility Map  
at the Hong Kong International Airport

P.W. Chan & C. M. Li

First International Conference on Sustainable Urbanization,  
15 – 17 December 2010, Hong Kong

## **CLIMATOLOGY AND PERFORMANCE OF LIDAR-BASED VISIBILITY MAP AT THE HONG KONG INTERNATIONAL AIRPORT**

P. W. Chan<sup>1</sup> and C. M. Li<sup>1</sup>

<sup>1</sup> Hong Kong Observatory, Hong Kong, China

### **ABSTRACT**

Visibility maps have been generated in real time at the Hong Kong International Airport (HKIA) based on the backscattered power data from Doppler LIght Detection And Ranging (LIDAR) systems and the visibility readings from the forward scatter sensors at the airport. The climatology of visibility at HKIA is studied in this paper by considering the mean visibility maps in different seasons and different years. The visibility is found to be the lowest in winter and the highest in summer. There appears to lower visibility areas to the north through west of HKIA, which may be related to the haze brought about by the north to westerly winds in northeast monsoon weather in the winter and the sea breeze.

Performance of the visibility map is also studied by considering the visibility maps based on the forward scatter sensors at the eastern and central parts of HKIA and using the sensors at the western part of the airport to provide independent measurements for verification purpose. Based on box plots, the visibility maps are found to have generally satisfactory quality, especially for visibility of 1500 m or above.

In the past studies, the LIDAR-based visibility map is mostly used to study haze and mist weather. Its performance in a fog case in 2005 is studied in the present paper.

### **KEYWORDS**

LIDAR, backscattered power, forward scatter sensor, visibility, box plot.

### **INTRODUCTION**

The Doppler LIDARs at HKIA are mainly used for monitoring windshear and turbulence to be countered by the landing/departing aircraft. The backscattered power data from the LIDARs are also found to be useful in the monitoring of low visibility weather. They have been used with the visibility readings from the six units of forward scatter sensor along the two runways of HKIA (locations in Figure 1) to generate visibility maps in real time, which could reach a maximum range of about 10 km from the LIDAR location. Technical details of the generation of such visibility maps could be found in Chan et al. (2007).

In the present paper, only the LIDAR at Air Traffic Control Complex near the centre of HKIA is considered, viz. before its relocation to the south runway of the airport.

### **VISIBILITY CLIMATOLOGY**

In studying the visibility climatology of HKIA, the visibility maps are generated from the LIDAR and all the 6 units of forward scatter sensors at the airport. Only the 1-degree conical scans are considered in this paper. In each season, the visibility data at each range gate and azimuth angle of the LIDAR are averaged using harmonic mean.

The climatological maps in different seasons and years are shown in Figure 2. For autumn 2005 (between September and November, Figure 2(a)), the visibility is rather uniform in the airport area and its value is mainly about 7 km. The visibility is slightly higher within about 1 km from the LIDAR which may be related to the optics of the LIDAR (Hannon, private communication). Similar artefacts of higher visibility near the LIDAR also show up in the visibility maps in other periods of time.

In the winter (Figure 2(b), between December 2005 and February 2006), the visibility is lower between 2 and 6 km from the LIDAR to the north through west of HKIA. This may be related to the haze brought from the northern and western parts of Pearl River Estuary by the northeast monsoon and the westerly sea breeze. The visibility is higher at distances of more than 6 km away, which may be due to the less polluted air higher up in the boundary layer of the atmosphere. At a distance of 6 km from the LIDAR, the laser beam is around 150 m above mean sea level.

In the spring (Figure 2(c), between March and May 2006), the lower visibility region to the north and northwest of HKIA continues to exist. The visibility is rather high (about 9 – 10 km) at distances of 6 km away from the LIDAR. This may be related to the small amount of LIDAR data available at such distances as a result of the low cloud base and the occurrence of fog/mist weather in the spring. In the summer (Figure 2(d), between June and August 2006), the visibility is generally very high (above 10 km) in the airport area. Note that the colour scale of visibility in Figure 2(d) is different from those in Figures 2(a) to (c).

The visibility climatology of the following year is also considered. Two representative climatological maps are shown in Figures 2(e) (September to November 2006) and (f) (December 2006 to February 2007). Once again, the visibility is generally uniform and around 7 km in the autumn, and there exists an area of lower visibility to the north through west of the airport in the spring. The visibility patterns are very similar to those of the previous year.

Though there are a couple of artifacts in the visibility climatological maps, namely, higher visibility the first couple of km from the LIDAR due to optics of the instrument and the visibility of about 9 km at far ranges in the spring-time map due to limited availability of LIDAR data, such maps depict interesting features of the seasonal and spatial variation of the visibility around HKIA, which could not be obtained from other data sources, e.g. point measurements from visibility sensors and aerosol optical depth (AOD) maps of coarser resolution from satellites.

## **PERFORMANCE OF VISIBILITY MAP**

Independent visibility data would be required to study the performance of visibility maps. For this purpose, the maps are generated based on the four forward scatter sensors at the eastern and centre parts of HKIA only, and the two sensors at the western part of HKIA are used to provide independent visibility readings for verification purpose. The performance is examined using box plot of the ratio of LIDAR-estimated visibility values at the locations of the latter two sensors and the actual sensor readings. This ratio is compared with the operationally desirable accuracy of meteorological optical range as given in ICAO (2007). The resulting box plots between December 2004 and January 2008 are shown in Figures 3(a) and (b). It could be seen that the LIDAR-based visibility estimates are of generally satisfactory quality, particularly for visibility of 1500 m or above. In this range of visibility, the 25 to 75 percentiles of the ratio generally lie within the accuracy requirement. For lower visibility, it appears that the LIDAR-estimated visibility tends to be higher than the forward scatter sensor value. This may be related to the higher altitude of the laser beam at the sensor location (about 100 m above ground). In view of the different sampling volumes of the LIDAR (100 m long) and the forward scatter sensor (several tens of centimeters), the comparison result for the two visibility datasets is considered to be good.

## **OBSERVATIONS IN A FOG CASE**

In Chan et al. (2007), observations of the visibility maps in haze and mist cases have been considered. It turns out that the map is also useful in the monitoring of the dispersion of fog. One such case occurred in the early morning of 8 February 2005. Fog with a visibility as low as 300 m was reported at 7 a.m. on that day by the weather observer at HKIA. Visibility map at that time (Figure 4(a)) showed that the visibility was mostly below 1 km in the airport area. Due to rapid attenuation of the laser beam in the suspending water in the air, LIDAR data were generally not available at the western part of HKIA. A picture taken by the weather observer at that time showed that fog was affecting the region (Figure 4(b)). After sunrise, fog dispersed gradually and the visibility given by the weather observer rose to 6 km in the following hour. Visibility map showed significant improvement of visibility over HKIA (Figure 4(c)), though the visibility remained at about 3 km at the western part of the airport. The occurrence of shallow mist in that area was confirmed by a photo (Figure 4(d)). It could be seen from the present case that, though some LIDAR data may not be available when HKIA is well within dense fog, the LIDAR-based visibility map is at least useful in the monitoring of the dispersion of the fog.

## CONCLUSIONS

This paper describes an algorithm to generate visibility map using the backscattered power data from a Doppler LIDAR and the visibility measurements from a limited number of forward scatter sensors within the coverage of the LIDAR. The visibility maps so obtained are found to reveal many interesting features of the variation of visibility in the vicinity of HKIA. They could be applied to different kinds of low visibility weather, such as mist and haze. Compared to in situ visibility measurements, for instance, from forward scatter sensors, the LIDAR-based visibility maps greatly extend the monitoring area and would be useful in the short-term forecasting of low visibility conditions for aviation and other applications. Of course, due to rapid attenuation of the laser beam in very humid air, the visibility map will have limited application value in fog and heavy rain.

The LIDAR-based visibility maps are used to establish the seasonal and spatial variation of visibility in the vicinity of HKIA. They are of good quality by comparing with independent forward scatter sensor readings based on box plots. Despite rapid attenuation of laser beam in suspending water in the air, the maps could at least be useful in the monitoring of dispersion of dense fog, as shown in a case study in the present paper.

## ACKNOWLEDGMENTS

The authors would like to thank Dr. A.Y.S. Cheng and Mr. R.L.M. Chan for developing the algorithm of LIDAR-based visibility map when they worked in the City University of Hong Kong between 2004 and 2006.

## REFERENCES

- Chan L. M., P. W. Chan, Y. S. Cheng, 2007: Generation of Visibility Map at the Hong Kong International Airport (HKIA) using LIDAR data, *Third Symposium on Lidar Atmospheric Applications*, American Meteorological Society.
- ICAO, 2007: Meteorological Service for International Air Navigation, Annex 3 to the Convention on International Civil Aviation, 187 pp.

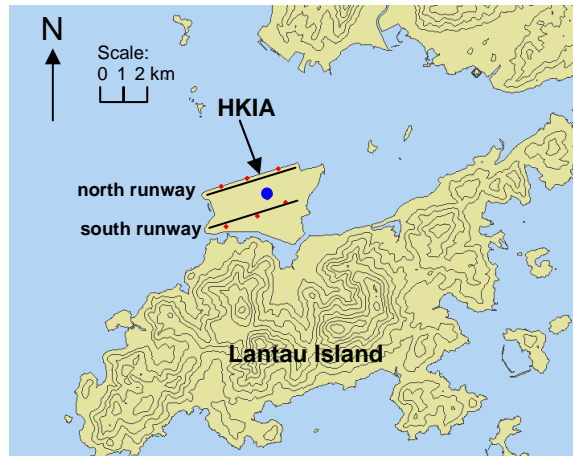


Figure 1 Locations of the LIDAR (blue) and forward scatter sensors (red) at HKIA.

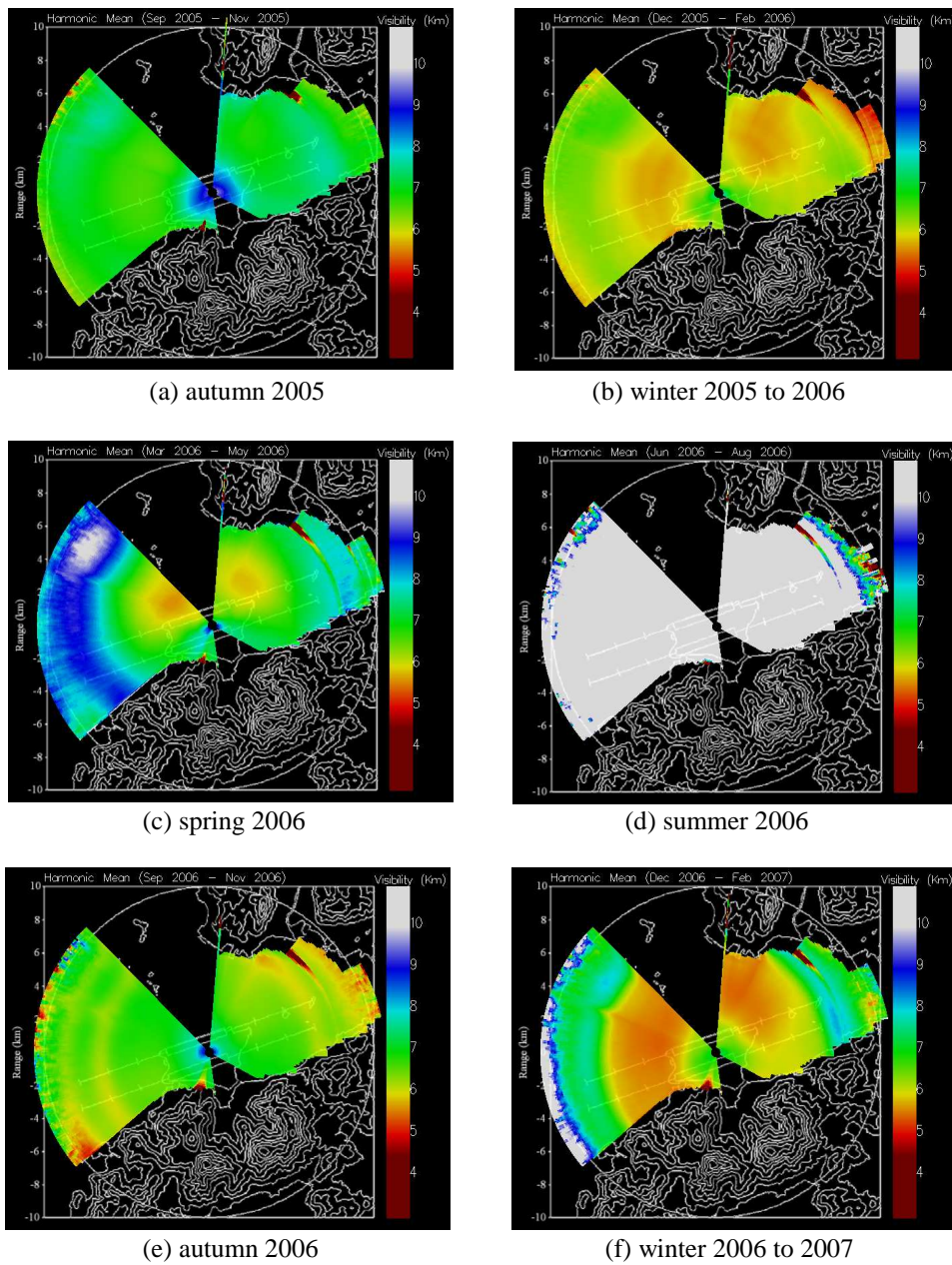
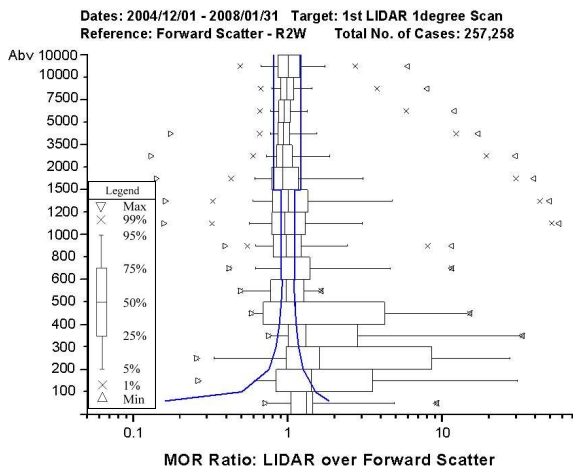
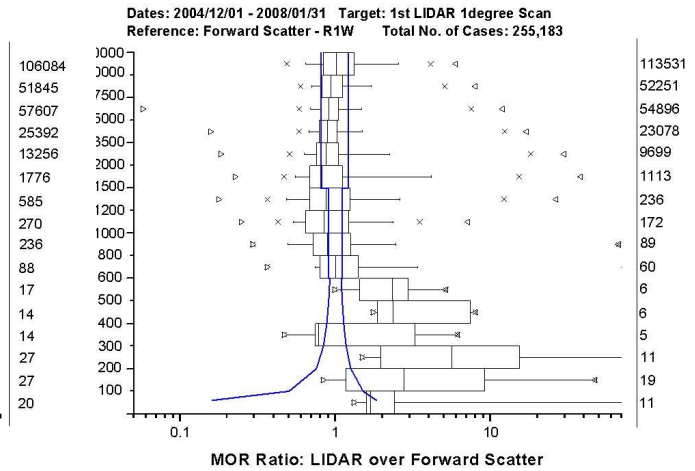


Figure 2 The (harmonic) average visibility maps at different seasons.

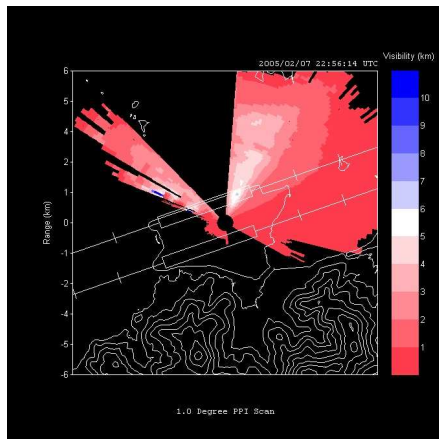


(a) box plot for western end of north runway



(b) box plot for western end of south runway

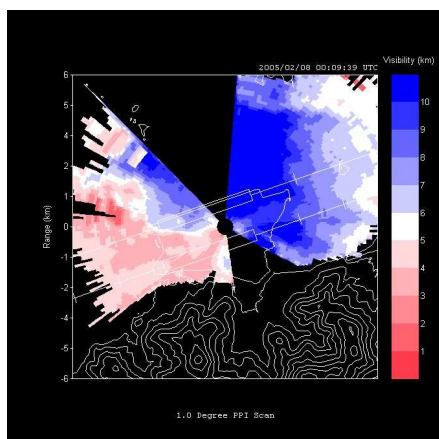
Figure 3 Box plots for visibility (LIDAR over forward scatterer) for western ends of the two runways.



(a) visibility map at about 6:56 a.m.



(b) photo taken to north-northwest at about 7 a.m.



(c) visibility map at about 8:10 a.m.



(d) photo taken to the northwest at about 8 a.m.

Figure 4 LIDAR-based visibility maps (a) and (c) and photos taken at the airport meteorological office near the centre of HKIA (b) and (d) for the fog event in the morning of 8 February 2005.